Current-Induced Magnetization Switching and CPP-GMR in 30 nm ϕ Scale Spin Valves Fabricated Using EB-Assisted CVD Hard Masks

Shinji Isogami[1], Masakiyo Tsunoda[1], and Migaku Takahashi[1,2]

[1]Department of Electronic Engineering, Tohoku University, Sendai 980-8579, Japan
[2]New Industry Creation Hatchery Center, Tohoku University, Sendai 980-8579, Japan

In this study, current-perpendicular-to-plane great magnetoresistance (CPP-GMR) spin valves with the minimum pillar width of 34 nm ϕ were successfully fabricated using EB-assisted chemical–vapor–deposition (CVD) hard masks. An area of the obtained magnetic cell is about one order smaller compared with those fabricated with normal EB or photo lithography technique. Measurement of transport properties such as current-induced magnetization switching (CIMS) and MR were demonstrated in such spin valves with various pillar widths. Dependence of the CPP-MR properties on the milled pillar width was discussed. In the case of 66 nm ϕ width in particular, the MR by external magnetic field switching and CIMS were 0.4% and 0.3%, respectively. The critical switching current I_c was $\sim$40 mA ($J_c \sim 9 \times 10^8$ A/cm^2). In the case of smaller width, only MR by external magnetic field was observed.

Index Terms—**Chemical–vapor–deposition (CVD), CPP-GMR spin valve, critical current density, current-induced magnetization switching (CIMS), electron beam (EB), magnetoresistance (MR), scanning electron microscope (SEM).**

I. INTRODUCTION

IT is well known that current-induced magnetization switching (CIMS) is a promising technique to realize high-density magnetic-random-access memories (MRAMs) from a viewpoint of power consumption. Moreover, magnetization precession effect has been also observed by spin transfer torque during current injection and such the effect is expected to be utilized in self-oscillation microwave devices for short-distance communication [1]. In order to reduce the operating current in such new devices, smaller spin valve is indispensable. EB lithography has been widely used as a sub-micron fabrication technique, of which achievable smallest cell size are 85×150 nm^2 [2], 100×200 nm^2 [3], 125×205 nm^2 [4], and so on. However, since deformation of patterned resist due to humid or high room temperature comes to be serious in nano-scaled fabrication, it is considered to be difficult to fabricate into smaller size such as several 10 nm. While a hard mask method is also developed for fabrication of CPP-GMR spin valves and magnetic tunnel junctions (MTJs) instead of resist mask method [5]–[7], EB resist should still be used for patterning of hard masks. In order to overcome such issues, the authors have developed the EB-assisted chemical–vapor–deposition (CVD) hard mask method without EB resist and have reported that by using this method, MTJ with the minimum pillar width of 80 nm ϕ could be achieved and reasonable MR properties were obtained [8]. In this study, both CIMS observation and MR measurement were demonstrated in CPP-GMR spin valves with nominal size of 30–120 nm ϕ fabricated using EB-assisted CVD hard masks.
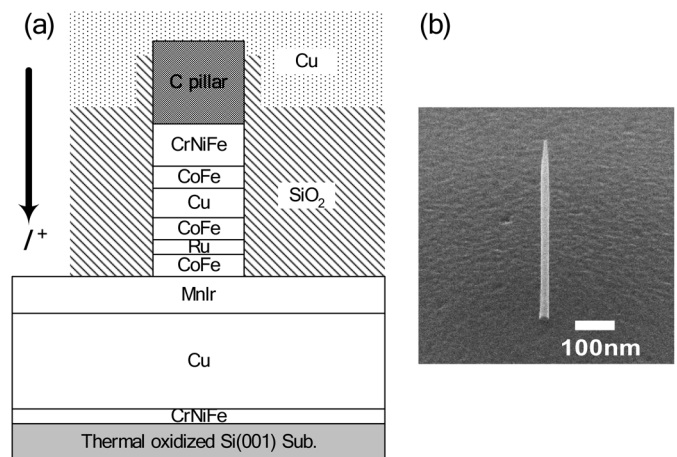
Fig. 1. (a) Schematic drawing of fabricated CPP-GMR spin-valve structure. (b) 52° tilted SEM image showing carbon pillar (30 nm $\phi \times$ 700 nm) hard mask just after deposited onto the GMR film surface.

II. EXPERIMENTAL PROCEDURE

A. Film Preparation and Fabrication

CPP-GMR spin valve film, showing in Fig. 1, thermal-oxidized Si substrate/bottom electrode/Mn$_{75}$Ir$_{25}$(10)/Co$_{70}$Fe$_{30}$(4)/Ru(0.9)/Co$_{70}$Fe$_{30}$(4)/Cu(5)/Co$_{70}$Fe$_{30}$(4)/Cr$_{66}$Ni$_{24}$Fe$_{10}$(10) (in nm) was stacked using DC magnetron sputtering system, of which base pressure was less than 9×10^{-9} Torr. A Cr$_{66}$Ni$_{24}$Fe$_{10}$(5)/Cu(500) was stacked as the bottom electrode. To flatten the surface of thick Cu layer, *in situ* 250 °C IR heat treatment was applied before MnIr deposition [9]. Carbon was selected for hard mask material and deposited onto full-stacked GMR film surface. The carbon pillar acts not only as a milling mask but also as a top electrode for the MR measurement. The width of carbon pillar was varied from 30

to 120 nm by adjusting the acceleration voltage, diameter of EB, and carbonic gas pressure. The shape of carbon pillar is determined by EB scanning in our technique. In order to obtain the smallest junction area, EB was not scanned in this experiment and circular-shaped carbon pillar was formed. Carbon pillar height was fixed at 700 nm. Then, in order to maintain antiferromagnetical coupling in the CoFe/Ru/CoFe trilayer by adjusting the volume of both CoFe layer, GMR film was etched down to the interface between MnIr and pinned CoFe layer by Ar ion. After etching, a circular-shaped CPP-GMR spin valve was formed. Junction area was defined as the contact area of top carbon mask electrode. Field annealing at 300 °C under 1 34kOe was applied on the nano-fabricated samples for 1 h. Since more detailed fabrication procedure is given in [8], we only mentioned the outlines here.

B. Measurement of MR Properties and CIMS Observation

MR properties were measured using the dc-4-probe method at room temperature. To observe the CIMS phenomena, pulsed switching current with 0.5-mA steps, a 400-ms interval and 1000-ms duration was applied perpendicular to the GMR film from -120 mA to $+120$ mA. Then, device resistance was measured during the each interval with read current of 1 mA. The sign of an injected current was defined as positive when electrons flew from the reference layer (a pinned layer) to the magnetization switching layer (a free layer).

III. RESULTS AND DISCUSSION

A. Junction Area Dependence of CPP-MR Properties

Fig. 2 shows the resistance (R) of fabricated CPP-GMR spin valve. It is noteworthy that possible fabrication area using our developed EB CVD method is one order smaller than that using conventional EB lithography. While each plot is scattered by dispersion owing to fabrication process A dependence of R is generally observed. In order to confirm absolute value of such R, calculation based on the $R = \rho \times (L/S)$ relationship was carried out, where ρ is treated as the series connected resistivity of each layer of GMR stacks and interfaces. The resistivity of each material was determined as an actually measured in-plane value of thick-monolayer sample. They are $(\rho_{\mathrm{CrNiFe}}, \rho_{\mathrm{CoFe}}, \rho_{\mathrm{Cu}}$ and $\rho_{\mathrm{Ru}}) = (1407, 117, 19$ and 107 m$\Omega\mu$m), respectively. $\rho_{\mathrm{carbon\ pillar}}$ was determined as 16 400 m$\Omega\mu$m referring to bulk carbon resistivity. The resistivity of each interface which are $\rho_{\mathrm{(CrNiFe,CoFe)}}, \rho_{\mathrm{(Cu,CoFe)}}, \rho_{\mathrm{Ru,CoFe}}$, and $\rho_{\mathrm{MnIr,CoFe}}$) were determined from the RA product given in [10]. L is a milled depth of 27.9 nm and S is a junction area (A). As a result, ρ including carbon resistance was calculated as 13 443 m$\Omega\mu$m. The broken line in Fig. 2 provides R with this ρ; however, the measured data are located for below of it. When the carbon resistance was ignored in the above calculation, ρ was calculated as 561 m$\Omega\mu$m. The solid line in Fig. 2, for this case, seems to agree with the measured data. This fact implies that sense current does not conduct through a carbon pillar in the present system and might conduct through another
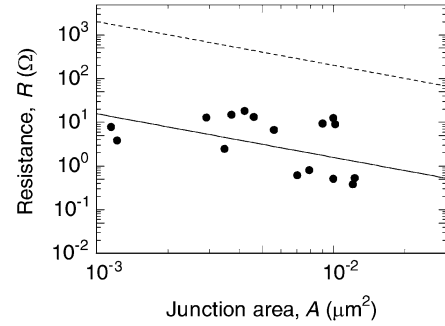

Fig. 2. Closed circles are measured data showing junction area (A) dependence of fabricated CPP-GMR spin-valve resistance (R). Solid line shows calculation based on $R = \rho \times (L/S)$ relationship except for carbon pillar resistance. Broken line shows one including carbon pillar resistance.
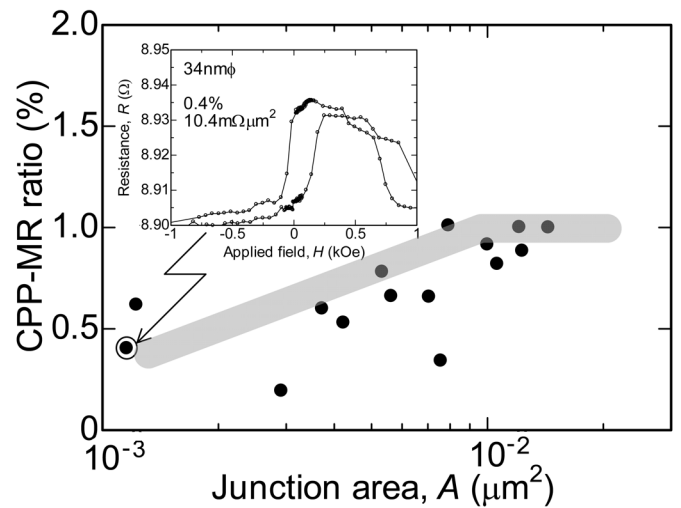

Fig. 3. Closed circles are measured data showing junction area (A) dependence of CPP-MR ratio. The inset shows R–H curve of the CPP-GMR spin valve with minimum width of 34 nmϕ. Its MR and RA product were 0.4% and 10.4 m$\Omega\mu$m^2.

low-resistance current path formed on a side wall of carbon pillar.

Second, the CPP-MR properties as a function of A showing in Fig. 3 are discussed. Over $A = 0.01$ μm^2, which is corresponded to 100×100 nm^2 or so, CPP-MR was constantly 1%. While CPP-MR reduces gradually as A reduces, an MR ratio of 0.4% and an RA product of 10.4 m$\Omega\mu$m^2 are successfully obtained even at the achieved minimum $(A)^{1/2}$ of 34 nm ϕ in this study. The obtained MR and RA product are one order smaller compared with another report [10]. The most possible reason is the formation of redeposited layer on pillar wall as mentioned above. Since the sense current that conducts in a GMR unit reduces, the CPP-MR ratio comes to be low. The other possibility of low RA and low MR is due to physical damages on a CPP-GMR spin-valve pillar during Ar ion milling. And their influences must be more and more dominate with decreasing A.

B. CIMS Observation

In CPP-GMR spin valves with down to 66 nm ϕ region, CIMS was successfully observed. Fig. 4 shows R–H and R–I curves of CPP-GMR spin valve with 66 nm ϕ. The CPP-MR ratio by
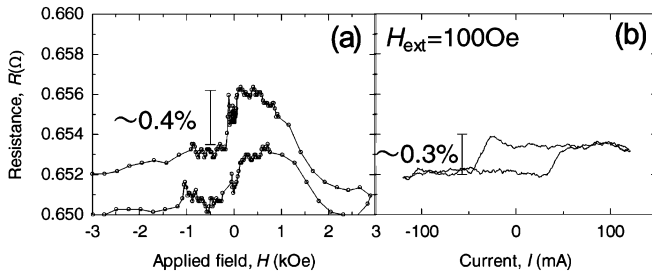
Fig. 4. (a) R–H curve and (b) R–I curve of the CPP-GMR spin valve with the pillar width of 66 nmθ.
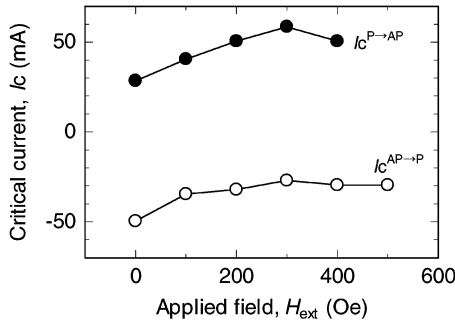

Fig. 5. Applied external field (H_{ext}) dependence of critical switching current (I_c). Closed and open circle with solid line are $I_c^{\text{P}\rightarrow\text{AP}}$ and $I_c^{\text{AP}\rightarrow\text{P}}$, respectively.

external magnetic switching and by CIMS under 100 Oe external field were ~0.4% and ~0.3%, respectively. The critical current $I_c^{\text{P}\rightarrow\text{AP}}$, where magnetization alignment of the free layer referring to the pinned layer switches from the parallel (P) to the antiparallel (AP) state, was ~40 mA, and $\Delta I_c(= I_c^{\text{P}\rightarrow\text{AP}} - I_c^{\text{AP}\rightarrow\text{P}})$ was ~80 mA. The average switching current density (J_c) was ~9×10^8 A/cm^2. In the cases of 70 nm ϕ and 80 nm ϕ, the J_c was $1.0 \sim 1.4 \times 10^9$ A/cm^2 and was not significantly different from the value in Fig. 4(b). The J_c of other junctions we obtained were almost similar. Fig. 5 shows critical switching current (I_c) as a function of applied external field (H_{ext}), measured for the CPP-GMR spin valve with 66 nm ϕ width. One can see that both of $I_c^{\text{P}\rightarrow\text{AP}}$ and $I_c^{\text{AP}\rightarrow\text{P}}$ are shifted toward the positive direction with H_{ext} increasing. Therefore, high to low (low to high) resistance transition behavior surely indicates magnetization switching of the free layer by spin transfer torque. However, our obtained I_c is one order larger than that of typical case [2]. According to the spin angular momentum transfer model proposed by Slonczewski for the CPP-GMR system [11], I_c can be expressed as follows:

$$I_{\text{c}} = e\alpha\gamma(H_{\text{ext}} \pm H_{\text{ani}} \pm M_s/2\mu_0)(M_sV/\mu_B)/g \quad (1)$$

where $g = \{-4 + (1/4)(P^{1/2} + P^{-1/2})^3(3 + \cos\theta)\}^{-1}$. Equation (1) does not assume the thermal activation by joule heat in this time. We consider that such large I_c is due to a large saturation magnetization of $Co_{70}Fe_{30}$ free layer of ~2.2 T or a large demagnetization field generated in a free layer. Because the fabricated CPP-GMR spin valve has a nominal circular

shape, the demagnetization field must be extremely large compared with that of elliptical shape. However, only such a large M_s value and a large demagnetization field cannot fully explain the large I_c. In order to find out the additional reason of large I_c, fitting of $I_c^{\text{P}\rightarrow\text{AP}} = +40$ mA and $I_c^{\text{AP}\rightarrow\text{P}} = -40$ mA were carried out independently using (1) and some parameters as follows: $\alpha = 0.009, H_{\text{ext}} = 7.96$ A/m, $H_{\text{ani}} = 19.9$ kA/m, $M_{\text{s}} = 2.2$ T, $V = 66 \times 66 \times 4$ nm^3. By varying the spin polarization (P) from 0.06 to 0.1, $I_c^{\text{P}\rightarrow\text{AP}} = +40$ mA and $I_c^{\text{AP}\rightarrow\text{P}} = -40$ mA were fitted well. This estimated P of a current passing through the CoFe layer was much smaller than the values of ~0.35, similar to the values of P measured in Co [12]. Judging from this fitting, the reason of such large I_c is considered to be the small P due to decreasing of CPP-MR in 66 nm ϕ region. Then, why is P estimated so small? The considerable reason is formation of redeposited layer on the pillar side wall. Since sense current mainly conducts through the side wall, intrinsic current that conducts through inside the GMR unit is reduced. In order to observe CIMS phenomena observation in less than the 66 nm ϕ region, further refinement of the nano-fabrication process is needed.

IV. SUMMARY

The 30 nm-scale pillar fabrication in CPP-GMR spin valves was demonstrated using EB-assisted CVD carbon mask. In this study, CPP-MR measurement and CIMS are carried out on the fabricated CPP-GMR spin valves with various pillar width. CPP-MR was successfully observed down to 34 nm ϕ. CPP-MR of 0.4% and 10.4 m$\Omega\mu$m^2 were obtained. On the other hand, CIMS was successfully observed down to 66 nm $\phi \cdot J_c \sim= 9 \times 10^8$ A/cm^2 and CPP-MR of 0.3% were observed.

REFERENCES

[1] S. I. Kiselev, J. C. Sankey, I. N. Krivorotov, N. C. Emley, R. J. Schoelkopf, R. A. Buhrman, and D. C. Ralph, *Nature*, vol. 425, pp. 380–383, 2005.
[2] K. Yagami, A. A. Tulapurkar, A. Fukushima, and Y. Suzuki, *Appl. Phys. Lett.*, vol. 85, pp. 5634–5636, 2004.
[3] H. Kubota, A. Fukushima, Y. Ootani, S. Yuasa, K. Ando, H. Maehara, K. Tsunekawa, D. D. Djayaprawira, N. Watanabe, and Y. Suzuki, *Jpn. J. Appl. Phys.*, vol. 44, pp. L1237–L1240, 2005.
[4] Z. Diao, D. Dmytro, M. Pakala, Y. Ding, A. Panchula, and Y. Huai, *Appl. Phys. Lett.*, vol. 87, p. 232 502, 2005.
[5] Y. Ding, M. Pakala, P. Nguyen, H. Meng, Y. Huai, and J. P. Wang, *J. Appl. Phys.*, vol. 97, p. 10C702, 2005.
[6] T. Niizeki, H. Kubota, Y. Ando, and T. Miyazaki, *J. Appl. Phys.*, vol. 97, p. 10C909, 2005.
[7] T. Okada, H. Kimura, I. Nunokawa, N. Yoshida, K. Etoh, and M. Fuyama, *IEEE. Trans. Magn.*, vol. 40, pp. 2329–2331, 2004.
[8] S. Isogami, M. Tsunoda, and M. Takahashi, *IEEE Trans. Magn.*, vol. 41, pp. 3607–3609, 2005.
[9] K. Imakita, M. Tsunoda, and M. Takahashi, *J. Magn. Soc. Japan.*, vol. 28, pp. 368–371, 2004.
[10] Y. Jiang, S. Abe, T. Nozaki, N. Tezuka, and K. Inomata, *Phys. Rev. B*, vol. 68, p. 224 426, 2003.
[11] J. C. Slonczewski, *J. Magn. Magn. Mater.*, vol. 159, pp. L1–L7, 1996.
[12] S. K. Upadhyay, R. N. Louie, and R. A. Buhrman, *Appl. Phys. Lett.*, vol. 74, p. 3881, 1999.